Electronic Supplementary Information

A bioscaffolding strategy for hierarchical zeolites with a nanotube-trimodal network

Guannan Li,[a] Haibo Huang,[a] Bowen Yu,[b] Yun Wang,[a] Jiawei Tao,[a] Yingxu Wei,[b] Shougui Li,[a] Zhongmin Liu,*[b] Yan Xu*[a] and Ruren Xu[a]

[a]*State Key Lab of Inorganic Synthesis and Preparative Chemistry, Jilin University, Changchun 130012, China. E-mail: yanxu@jlu.edu.cn*

[b]*National Engineering Laboratory for Methanol to Olefins, Dalian National Laboratory for Clean Energy, Dalian Institute of Chemical Physics, Dalian 116023, China. E-mail: liuzm@dicp.ac.cn*

Experimental

Materials

Dipotassium hydrogen phosphate (AR), anhydrous acetic acid (AR), sodium hydroxide (AR), ethanol (>99.7%, AR), ammonia solution (AR, 25-28%), isopropanol (AR) and tert-butanol (99%, AR) were purchased from Beijing Chemicals Reagent Company. Aluminum tri-sec-butoxide (ATSB, AR), tetraethyl orthosilicate (TEOS, AR, 99.9%) and polydiallyldimethylammonium chloride (PDDA, AR, Mw<100,000) were purchased from Aladdin Reagent (shanghai) Co Ltd. Chitosan (low molecular weight, 75-85% deacetylated) were purchased from Sigma Aldrich (Shanghai) Trading Co Ltd. D-glucose anhydrous (AMRESCO), peptone (AR, Beijing Aoboxing Biotechonology), yeast extract (OXOID), cetyltrimethyl ammonium bromide (CTAB, AR, 98.0%, Sinopharm Chemical Reagent Co Ltd), tetra-n-butyl titanate (TBOT, 98%, AR, Tianjin Guangfu Fine Chemical Research Institute), Rhodamine B (RhB, Guangfu Fine Chemical Research Institute), tetrapropylammonium hydroxide aqueous solution (TPAOH, AR, 20 wt%, Shanghai Cainorise Chemicals Co Ltd) were also used. Acetobacter xylinum HN001 was provided by Tianjin University, China. All chemicals were used as received.

Preparation

BC aerogel. BC was prepared according to reported procedures.[1] In a typical procedure, a culturing medium was prepared from 25 g of D-glucose anhydrous, 10 g of peptone, 7.5 g of yeast extract, 10 g of dipotassium hydrogen phosphate and 1 L of deionized water. It was adjusted to pH = 5.0 using anhydrous acetic acid. Acetobacter xylinum was cultured in sterilized medium at 30 °C for 4 days and BC pellicle with the thickness of about 1-2 cm was formed. The BC pellicles were treated using 1 wt% aqueous solution of sodium hydroxide at 90 °C for 0.5 h, followed by repeated washing using distilled water to pH = 7. Next, the treated BC was solvent exchanged using tert-butanol. The solvent exchange was conducted at 30 °C for 6-7 h under gentle agitation, and each procedure was repeated three times using fresh solvent. BC aerogel was generated by lyophilization from the solvent exchanged BC. It has a porosity of 97 % and BET surface area of 123 m^2g^{-1}.

Ch hydrogel. Ch hydrogel was prepared according to reported procedures.[2] In a typical experiment, 2.5 g of chitosan powder was dissolved in 100 ml of acetic acid solution (0.055 $molL^{-1}$). The mixture was added dropwise to a sodium hydroxide solution (4 M) using a syringe with needle inner diameter of 0.8 mm. Ch hydrogel was well formed after 2 h of reaction in an alkaline medium, it was recovered by filtration and repeated washing with distilled water.

BC@aluminosilicate precursor scaffold (BC@ASO). In a typical experiment, 1.1 g of CTAB was added to 22.5 ml of ethanol under agitation till complete dissolution, to which 0.06 g of BC aerogel was added. 0.5~1 ml of ATSB in isopropanol (13 wt%) was added dropwise to above solution mixture after BC aerogel was fully swollen. The mixture was gently heated and stirred magnetically for 30 min to facilitate dissolution. Next, 2.3~4.5 ml of TEOS was added under agitation for 30 min. The solution mixture was cooled in an ice bath, followed by addition of 4.25 ml of ammonia solution. The mixture was agitated for 4 h to allow thorough hydrolysis and polycondensation. White precursor scaffold of BC@ASO was washed using ethanol. The process was repeated to achieve desired layer thickness. Finally, BC@ASO was recovered after repeated washing using ethanol and oven-dried at 60 °C for 2 h.

BC@titanosilicate precursor scaffold (BC@TSO). In a typical experiment, 1.1 g of CTAB was added to 22.5 ml of ethanol under agitation till complete dissolution. Then, 0.06 g of BC aerogel was added to the above solution to allow swelling, to which 0.1 ml of TBOT and 4.5 ml of TEOS were added under magnetic stirring for 30 min. The solution mixture was cooled in an ice bath, followed by the addition of 4.25 ml of ammonia solution. The solution mixture was agitated for 4 h and BC@TSO was recovered after repeated washing using ethanol and oven-dried at 60 °C for 2 h.

BC@silicate precursor scaffold (BC@SO). In a typical experiment, 1.1 g of CTAB was added to 22.5 ml of ethanol under agitation till complete dissolution. Then, 0.06 g of BC aerogel was placed in the above solution to let the BC aerogel swell. 4.5 ml of TEOS was added to the above solution mixture and stirred for 30 min. Then, the solution mixture was cooled in an ice bath, to which 3.25 ml of ammonia solution was added. The mixture was agitated for 4 h to allow thorough hydrolysis and polycondensation. A white precursor scaffold of BC@SO was recovered after repeated washing using ethanol and oven-dried at 60 °C for 2 h.

Ch@silicate precursor scaffold (Ch@SO). Ch hydrogel was solvent exchanged using ethanol for three times. 3 g of the solvent-exchanged chitosan was immersed in 30 ml of ethanol solution containing TEOS at 50% (v/v). The solution was stirred gently for 12 h. It was filtered and then transferred to a 19% (v/v) ammonia/ethanol solution. The solution mixture was agitated for 4 h, and a white precursor scaffold of Ch@SO was recovered after repeated washing using ethanol and distilled water.

Sil-1 seeds. Sil-1 crystal seeds were prepared according to the reported procedures.[3] In a typical experiment, 16 g of TEOS was mixed with 27.32 g of TPAOH and stirred at room temperature for 24 h. The mixture was refluxed at 80 °C for 96 h, and colloidal crystals with uniform dimension of approximately 50 nm. It was recovered by centrifugation (12,000 rpm) and washed using deionized water repeatedly till pH ≈ 9.5. It was made into a 3 wt% aqueous solution.

Seeding of the BC@ASO, BC@TSO, BC@SO and Ch@SO precursor scaffolds. The precursor scaffolds were placed in a mixed aqueous solution of 0.5 wt% of PDDA and 0.5 M NaCl for 24 h, and washed using ammonia solution (pH = 10) for three times. Next, the treated scaffolds were impregnated in Sil-1 seed solutions at room temperature for 24 h to obtain seeded precursor scaffolds, then washed with ammonia solution (pH = 10) for three times to remove redundant seeds.

Vapor-phase transformation and calcination. The seeded precursor scaffolds were oven-dried at 60 °C for 2 h and placed on a polytetrafluoroethylene holder above a solution mixture of ethylenediamine (EDA), triethylamine (TEA) and water (H_2O) at a molar ratio of 1:12:13, and autoclaved at 140 °C for 72 h. ZNTS ZSM-5, TS-1 and Sil-1 were obtained after calcination at 550 °C for 5 h.

Characterization

Powder X-ray diffraction data (XRD) was recorded on Rigaku D/max 2550 X-ray diffractometer using Cu target radiation source (50 kV, 200 mA). Field emission scanning electron microscope (SEM) images were taken on JEOL JSM-6700F. The transmission electron microscopy (TEM) images were taken on a FEI Tecnai G2S-Twin with a field emission gun operating at 200 kV. The nitrogen (N_2) adsorption-desorption isotherms were recorded at 77.3 K with a Micromeritics ASAP 2420 surface area and porosity analyzer. Surface area was calculated by the Brunauer-Emmett-Teller (BET) method. Pore size distribution was calculated by the Barrett-Joyner-Halenda (BJH) method for mesopores and the Horvath-Kawazoe (HK) method for micropores using the adsorption branches of isotherms. Macroporosity was calculated based on the mercury (Hg) intrusion porosimetry measurements using a Micromeritics AutoPore IV system. Fourier transform infrared (FTIR) spectra were measured on Bruker IFS 66V/S spectrometer. Inductively coupled plasma spectroscopy (ICP) was performed on a Perkin Elmer OPTIMA 3300DV. The aluminum distribution across ZSM-5 nanocrystals was recorded on an ESCAlab 250 Analytical X-ray photoelectron spectrometer (XPS) using Ar-ion-sputtering technique. Each sputtering was 300s, capable of etching out 20-30 nm from surface. Temperature programmed desorption of ammonia (NH_3-TPD) was conducted on Micromeritics autochem II 2920 with a thermal conductivity detector (TCD) under helium flow. Before measurements, samples were converted to H-form by repeating the following process twice: ion-exchange with 1 M NH_4NO_3 aqueous solution (NH_4NO_3/Al = 10) and calcination at 500 °C for 3 h. UV-visible (UV-vis) spectra were measured using SHIMADZU U-4100 spectroscopy. Thermogravimetric (TG) analysis was carried out in air using NETZSCH STA 449 C instrument. ^{29}Si MAS NMR spectra were recorded on a 300 MHz Bruker Avance III spectrometer with an acquisition time of 7.5 ms, a recycle delay of 35 s, and an MAS rate of 6.5 kHz. ^{27}Al MAS NMR spectra were acquired at a 400 MHz Varian infinity plus 400 spectrometer with an acquisition time of 10 ms, a recycle delay of 0.6 s, and an MAS rate of 10 kHz. Laser scanning confocal microscopy images were taken on a Olympus FluoView FV1000 laser confocal microscope, before measurement the ZNTS ZSM-5 were prepared by dipping in 2 ppm rhodamine B solution and then dried on a microscope slide.

MTH conversion test

All catalysts were converted to H-form by repeating the following procedures twice: ion-exchange with 1 M NH_4NO_3 aqueous solution (NH_4NO_3/Al ≈ 10) and calcination at 500 °C for 3 h. The ZNTS ZSM-5 monolith was crushed and sieved to 40-60 mesh. For comparison, conventional ZSM-5 was prepared according to reported procedures.[4] MTH reactions were performed at 1 atm, 673 K and WHSV = 8 h^{-1} in He flow with a flow rate of 20 $mLmin^{-1}$. The catalyst was placed in a conventional fixed bed quartz tubular reactor. The products were analyzed using flame ionization detector (FID) and Aglient plot-Q column. The coke formation rate of the used catalysts was investigated using thermogravimetric analysis.

Notes and references

1 P. Wang, J. Zhao, R. Xuan, Y. Wang, C. Zou, Z. Zhang, Y. Wan and Y. Xu, *Dalton Trans.,* 2014, **43**, 6762.
2 F. Quignard, R. Valentin and F. D. Renzo, *New J. Chem.*, 2008, **32**, 1300.
3 B. Zhang, S. A. Davis, N. H. Mendelson and S. Mann, *Chem. Commun.,* 2000, 781.
4 R. V. Grieken , J. L. Sotelo, J. M. Menéndez and J. A. Melero, *Microporous Mesoporous Mater*., 2000, **39**, 135.

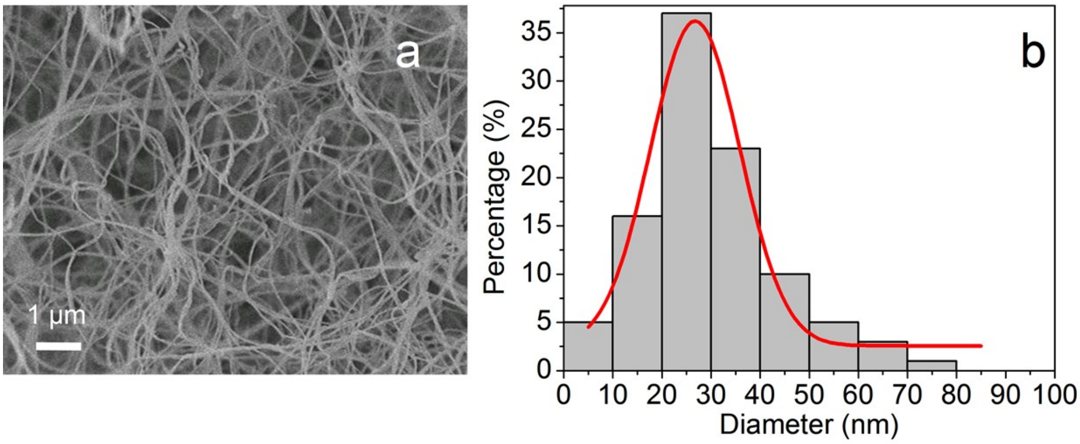

Fig. S1 Characterizing BC aerogel: (a) SEM. (b) Histogram of fiber diameter distribution.

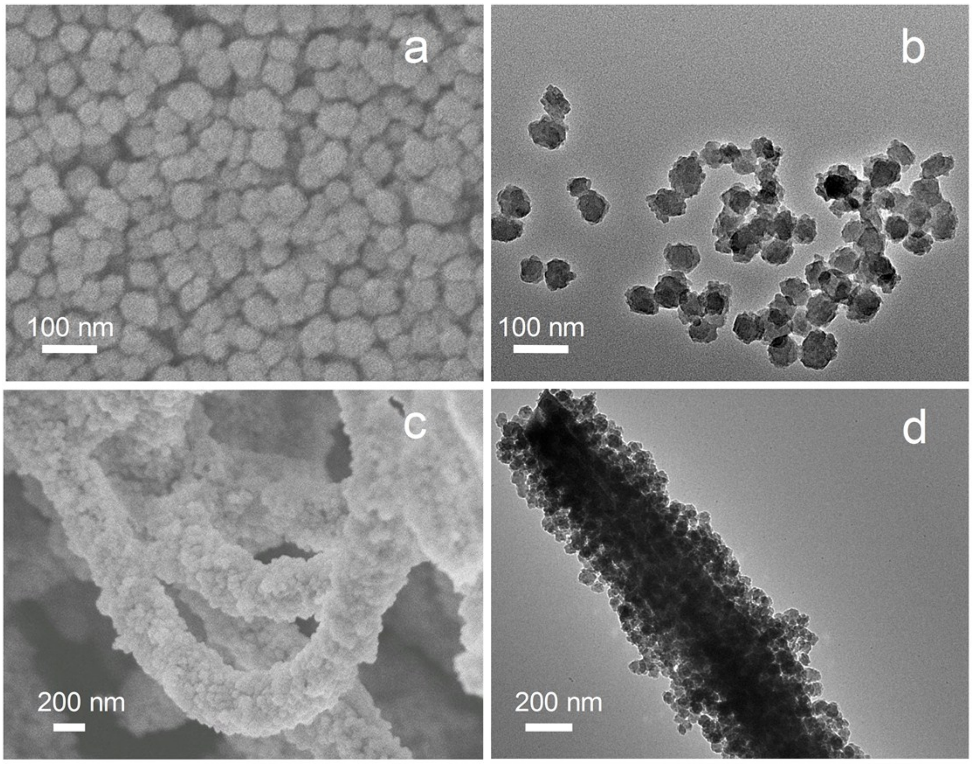

Fig. S2 (a) SEM of Sil-1 seeds. (b) TEM of Sil-1 seeds. (c) High magnification SEM of the Sil-1 seeded BC@ASO. (d) High magnification TEM of the Sil-1 seeded BC@ASO.

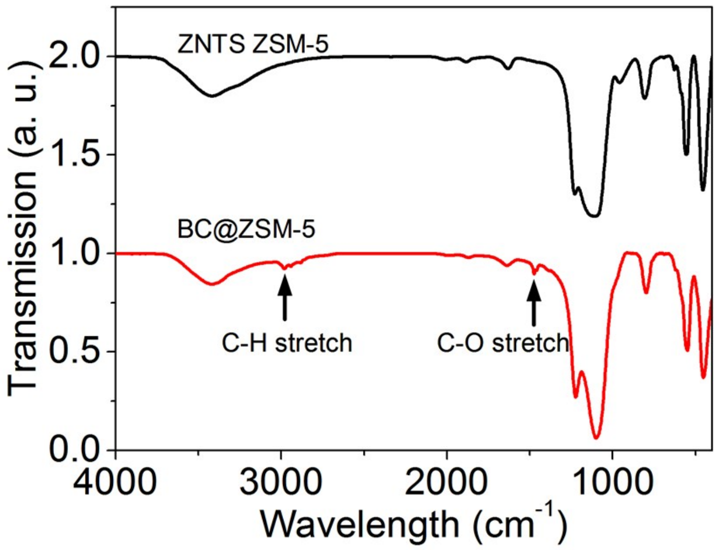

Fig. S3 FTIR spectra of BC@ZSM-5 and ZNTS ZSM-5. The peaks at 2970 cm^{-1} and 1062 cm^{-1} are assigned to the C-H stretching mode and C-O stretching mode of BC, respectively, indicating that BC is present in BC@ZSM-5 and absent in ZNTS ZSM-5.

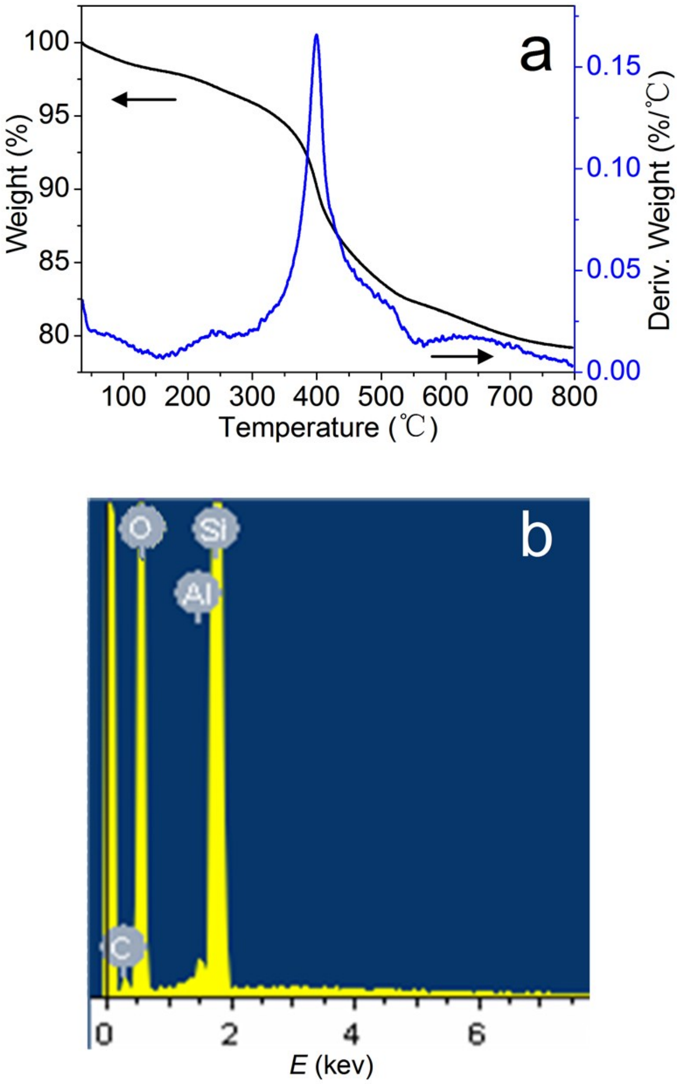

Fig. S4 (a) TGA/DTA of BC@ZNTS ZSM-5. (b) EDS analysis of ZNTS ZSM-5 showing negligible presence of carbon.

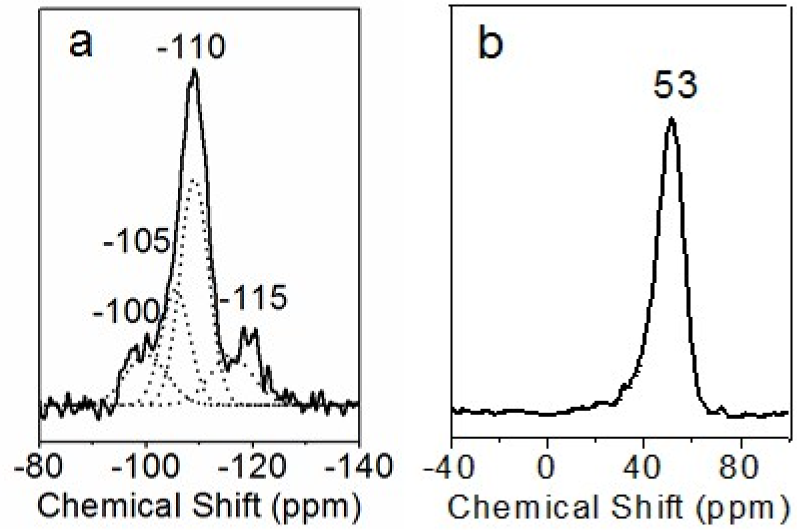

Fig. S5 Characterizing ZNTS ZSM-5: (a) ^{29}Si MAS NMR. (b) ^{27}Al MAS NMR.

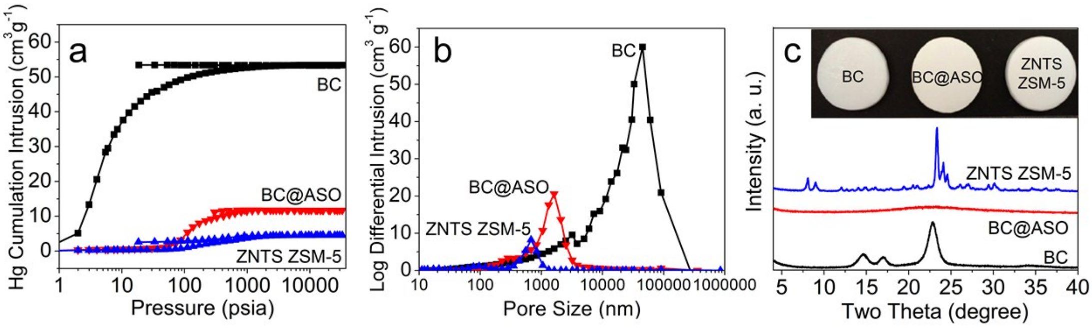

Fig. S6 (a) Hg intrusion porosimetry measurements. (b) Macropore size distribution. (c) XRD patterns of BC, BC@ASO and ZNTS ZSM-5 showing the loss of crystalline order of BC. Inset: Spongy disks of BC, BC@ASO and ZNTS ZSM-5 showing negligible volume changes throughout the nanofabrication process.

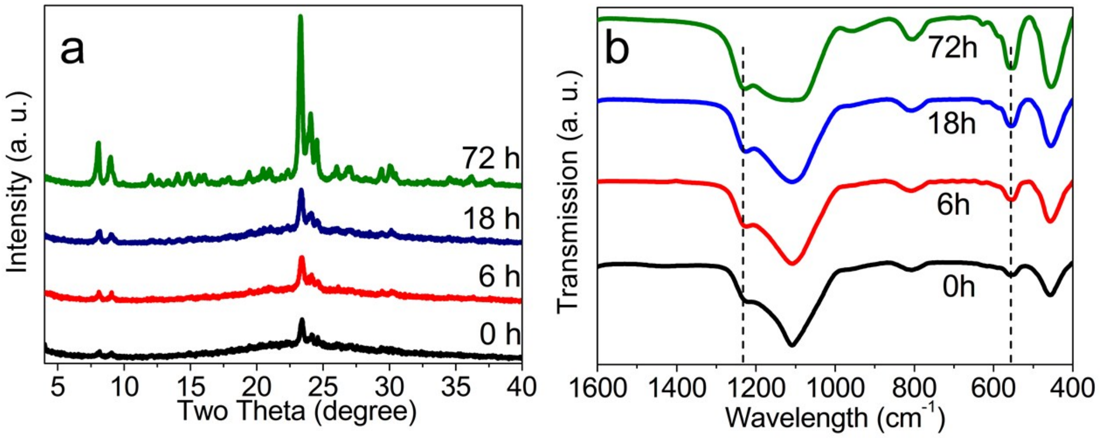

Fig. S7 Tracking the evolution of BC@ZSM-5 nanotube: (a) XRD. (b) FTIR.

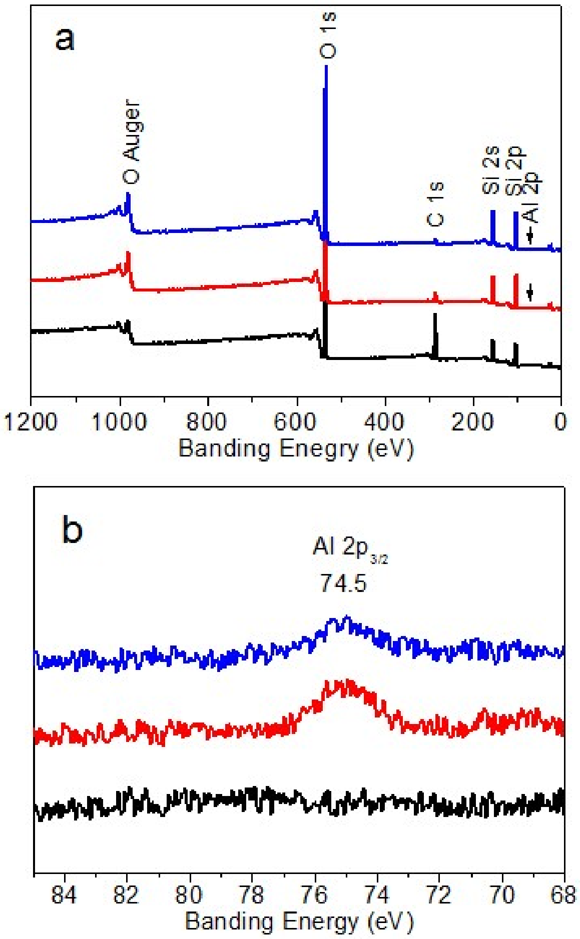

Fig. S8 XPS spectra of the Ar-ion-sputtered and untreated nanocrystals of ZSM-5 of ZNTS ZSM-5, and the Sil-1 seeds. (a) Survey spectra. (b) XPS peak of Al $2p_{3/2}$. Sil-1 seeds (black), untreated nanocrystals of ZSM-5 (red) and 300s sputtered nanocrystals of ZSM-5 (blue) of ZNTS ZSM-5.

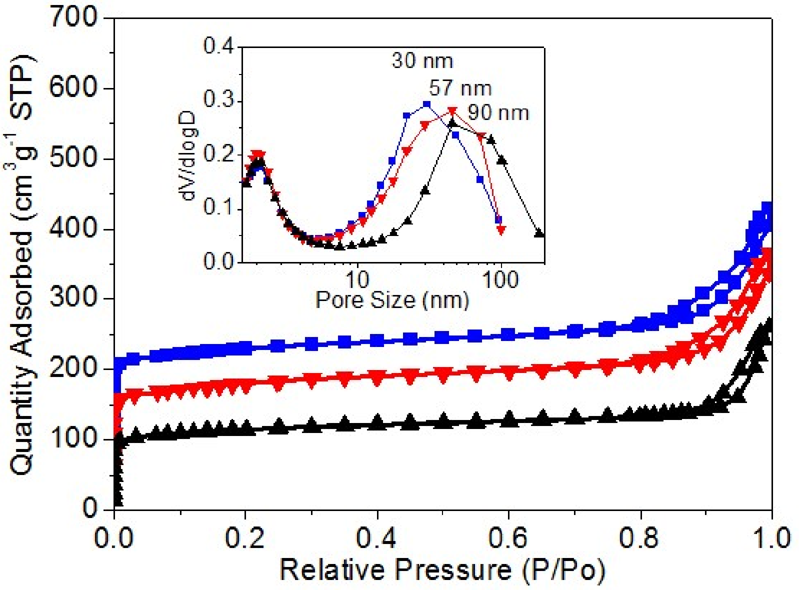

Fig. S9 N_2 adsorption-desorption isotherms of ZNTS ZSM-5 obtained from BC@ASO with varying thickness of the aluminosilicate layer. Inset: the inner diameter of the nanotubes of corresponding ZNTS ZSM-5.

Table S1. Textual properties of ZNTS ZSM-5 as a function of the thickness of the aluminosilicate layer.

Sample	BET Surface Area (m^2g^{-1})	Mesopore Surface Area (cm^3g^{-1})	Pore Volume (cm^3g^{-1})	Mesopore Volume (cm^3g^{-1})	Nanotube Inner Diameter (nm)
1	433.5	98.5	0.510	0.356	30
2	435.5	102.3	0.491	0.337	60
3	379.9	58.8	0.403	0.253	90

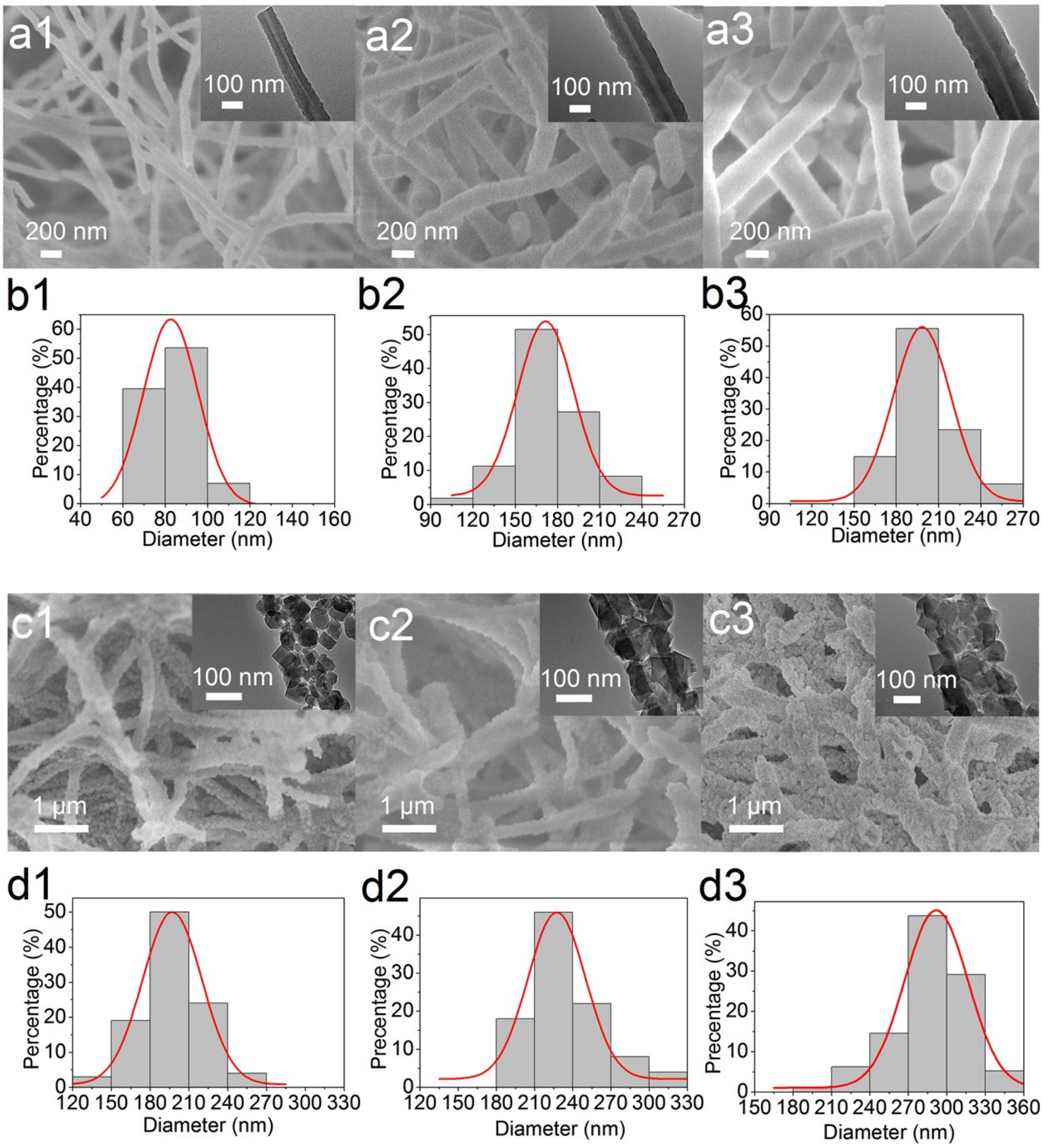

Fig. S10 (a) SEM of BC@ASO precursor scaffold with varying fiber diameter. Inset: Corresponding TEM showing the thickness of the aluminosilicate layer. (b) Corresponding histogram of fiber diameter distribution. (c) SEM of ZNTS ZSM-5 with varying nanotube outer diameter. Inset: Corresponding TEM showing the inner diameter of nanotubes. (d) Corresponding histogram of the nanotube diameter of ZSM-5 nanotubes.

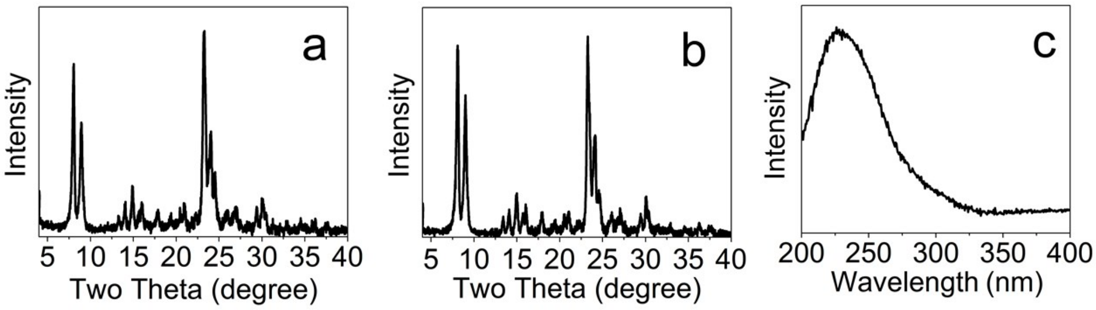

Fig. S11 (a) XRD pattern of ZNTS TS-1. (b) XRD pattern of ZNTS Sil-1. (c) UV-vis spectrum of ZNTS TS-1.

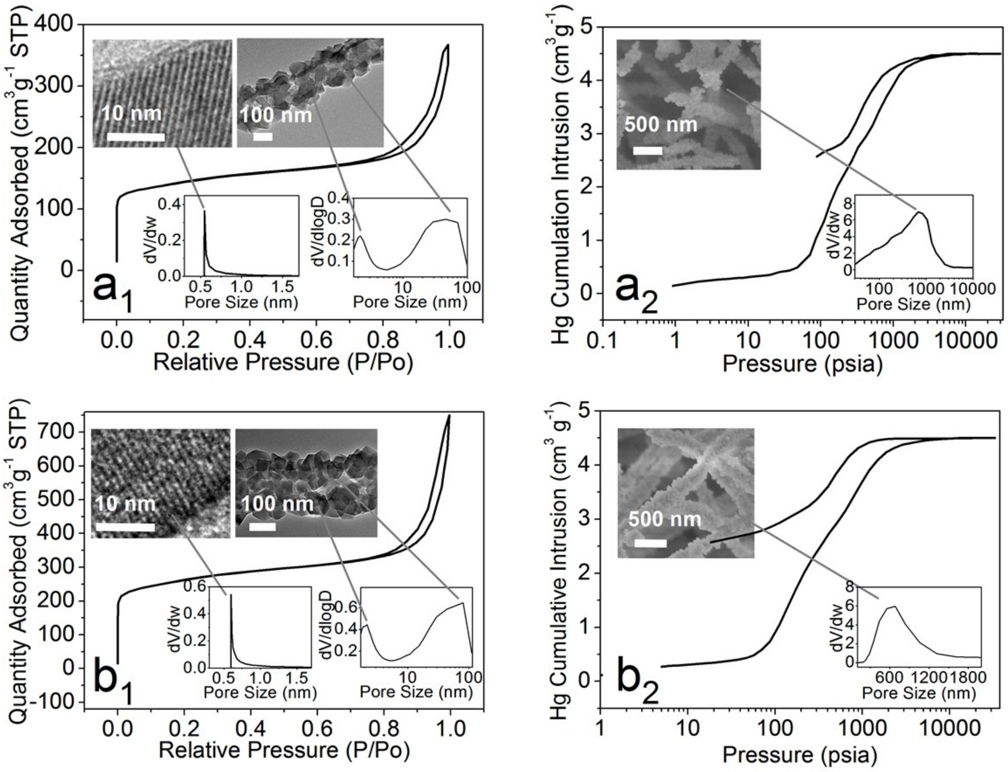

Fig. S12 Characterizing the porosity of ZNTS TS-1 (a) and ZNTS Sil-1 (b): (1) N_2 adsorption-desorption isotherm. Inset showing micropores, mesopores and nanotube. (2) Hg intrusion porosimetry measurements. Inset showing macropore profile.

Table S2. Textural properties of ZNTS TS-1 and ZNTS Sil-1.

Sample	BET Surface Area (m^2g^{-1})	Mesopore Surface Area (cm^3g^{-1})	Total Volume (cm^3g^{-1})	Nanotube Inner Diameter (nm)	Macropore Volume (cm^3g^{-1})	Porosity (%)	Median Pore Diameter (nm)
ZNTS TS-1	410.47	154.85	0.50	46	4.2	80.5	718
ZNTS Sil-1	482.93	198.51	0.57	80	4.5	84.5	678

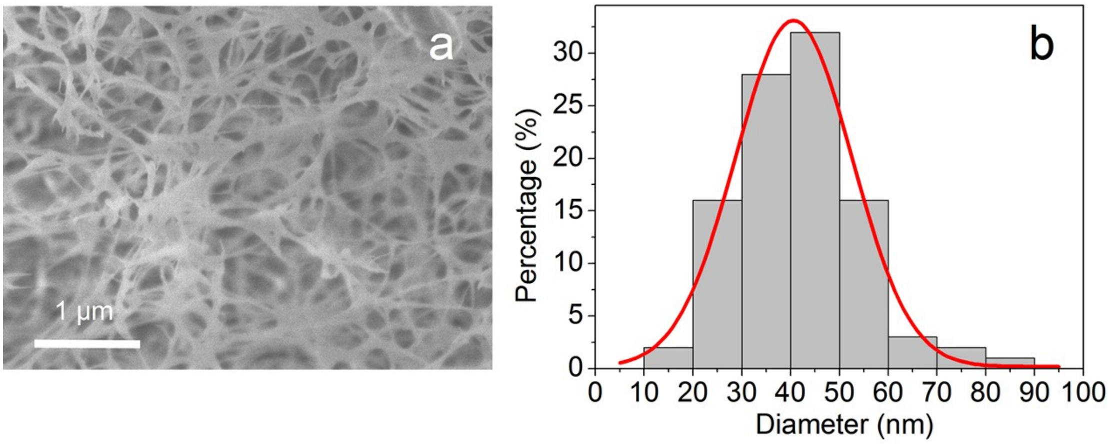

Fig. S13 Characterizing Ch aerogel: (a) SEM. (b) Histogram of fiber diameter distribution.

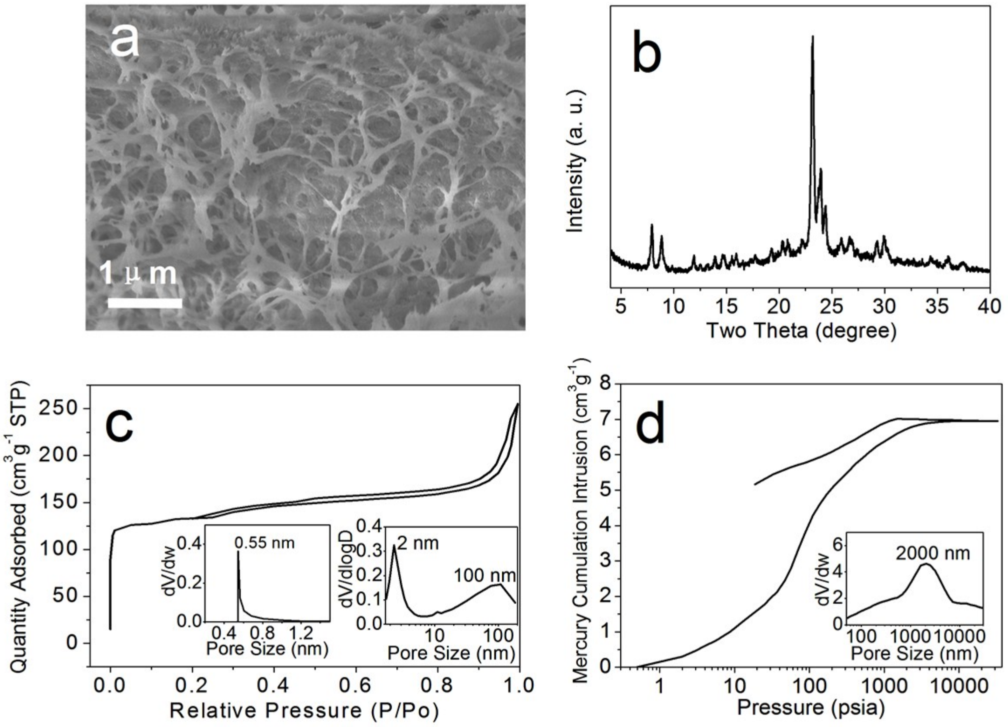

Fig. S14 Characterizing ZNTS Sil-1 (Ch): (a) SEM showing the scaffolding architecture. (b) XRD confirming MFI structure. (c) N_2 adsorption-desorption isotherm. Inset: micro-mesopore size distribution showing textural mesopores and nanotubes. (d) Hg intrusion porosimetry measurements. Inset: Macropore profile.

Table S3. Textural properties of ZNTS Sil-1 (Ch).

	BET Surface Area (m^{2}g^{-1})	Mesopore Surface Area (cm^{3}g^{-1})	Total Volume (cm^{3}g^{-1})	Macropore Volume (cm^{3}g^{-1})	Porosity (%)	Median Pore Diameter (nm)
ZNTS Sil-1 (Ch)	410.47	154.85	0.50	6.9	86.7	2000

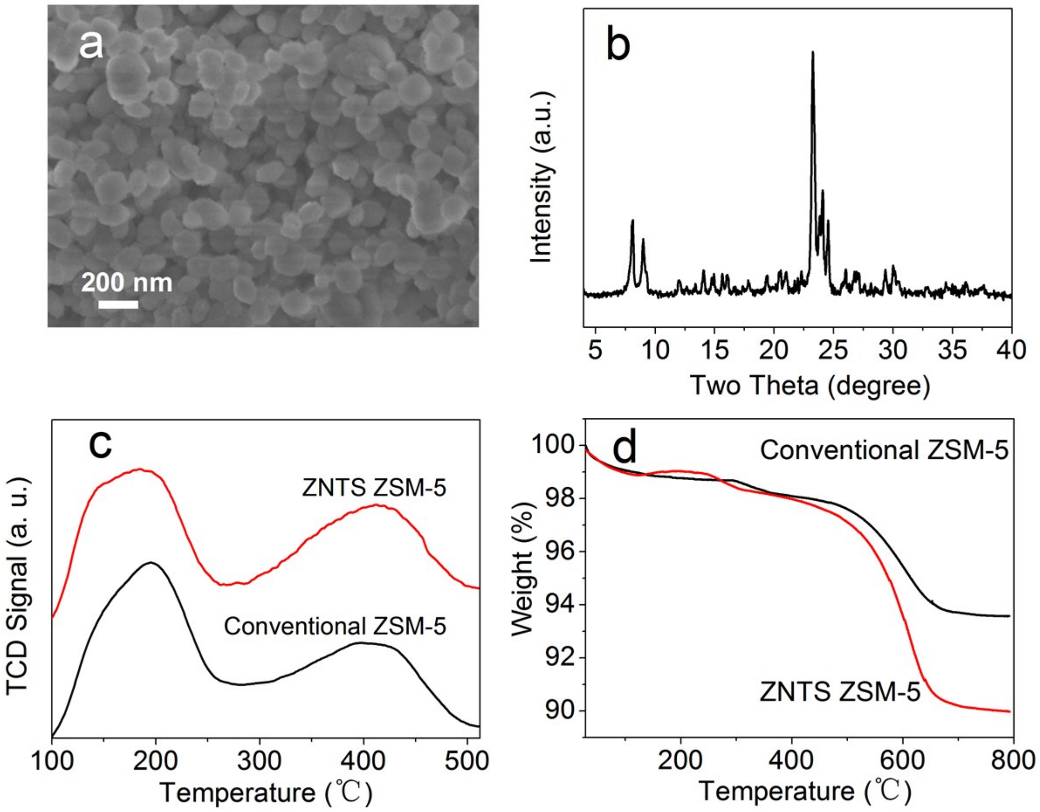

Fig. S15 (a) SEM of conventional ZSM-5 powder. (b) XRD pattern of conventional ZSM-5 powder. (c) NH_3-TPD profiles of ZNTS ZSM-5 and conventional ZSM-5 powder. (d) TG of used ZNTS ZSM-5 and conventional ZSM-5 powder after MTH reaction.

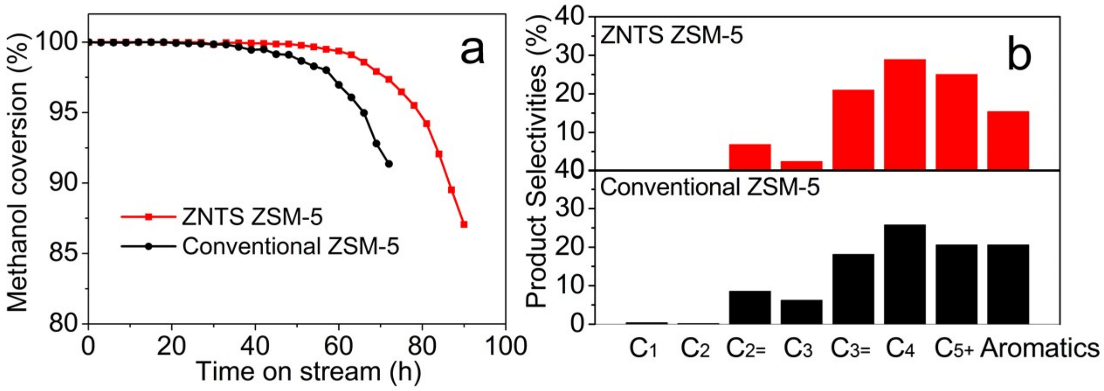

Fig. S16 (a) MTH conversion. (b) Hydrocarbon product selectivity. ZNTS ZSM-5 (red). Conventional ZSM-5 (black).